Arch. Min. Sci. **67** (2022), 1, 123-142

Electronic version (in color) of this paper is available: http://mining.archives.pl

DOI: https://doi.org/10.24425/ams.2022.140706

SRĐAN KOSTIĆ[1*], JELENA TRIVAN[2]

OPTIMIZATION OF COAL OVERBURDEN EXCAVATION CONSIDERING VARIABLE GEOMECHANICAL PROPERTIES AND STATES OF EXCAVATOR TEETH

We examine the impact of overburden geomechanical properties on the velocity of the excavator rotary movement V_b and on the excavator current consumption I_{max} for two different states of excavator teeth: new excavator teeth and worn-out teeth after minimum 250h of work. The analysed dataset is collected from recordings made by the bucket-wheel excavator SchRs 900 25/6 operating at "Tamnava Eastern field" open-pit coal mine in Serbia. The following geomechanical properties of the overburden are examined: grain size composition, unit weight, cohesion and angle of internal friction. Using multiple linear regression analysis, we develop explicit mathematical correlations between I_{max} and V_b and the overburden properties in a form of nonlinear equations for the case of new excavator teeth, while statistically significant correlation for the worn-out teeth is obtained only between overburden geomechanical properties and I_{max}. Results obtained indicate the existence of statistically significant two-factor interactions with positive effect of overburden unit weight and angle of internal friction on I_{max} and V_b, while cohesion is generally inversely proportional to the analysed outputs. Analysis performed enables optimized planning of the excavator performance regarding its productivity during the overburden excavation.

Keywords: current consumption; velocity of excavator rotary movement; excavator teeth; overburden properties; optimization

1. Introduction

Open-pit coal mining represents the main method of coal excavation in Serbia today. In general, history of coal excavation in Serbia could be divided into three periods. The first period lasted from the beginning of XX century to approximately 1965, when underground coal exploitation was dominant (coal mines Vrška čuka, Lubnica, Bogovina, Soko, Rembas, Jase-

[1] JAROSLAV ČERNI WATER INSTITUTE, SERBIA
[2] UNIVERSITY OF BANJA LUKA, FACULTY OF MINING PRIJEDOR, BOSNIA AND HERZEGOVINA
* Corresponding author: srdjan.kostic@jcerni.rs

novac, Ibarski mines, Štavalj and Aleksinački mines), with maximum production of 3.9 million tonnes in 1964. The second period was from 1965. to 1980. during which the coal production from underground exploitation had constantly been decreasing, while the coal production from open pits significantly increased (with the largest mines Kolubara, Kostolac, Kovin and Obilić). Number of underground coal mines decreased from 24 in 1965 to 14 in 1980. The third period started in 1980. and is still ongoing. During this period, open-pit coal mining is the dominant method of coal exploitation in Serbia, with the coal production of about million tonnes in 2000 Fig. 1a [1].

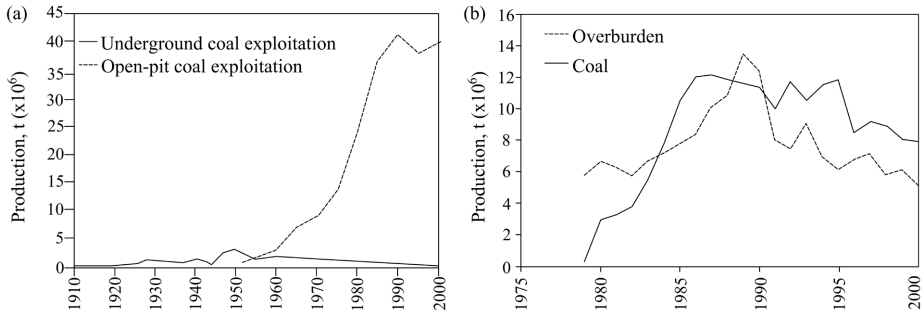

Fig. 1. (a) Coal production in Serbia, 1900-2000 [1], (b) Coal production at Tamnava Eastern Field, 1975-2000 [1]

There are different types of coal that have been exploited in Serbia: from lignite (Kolubara and Kostolac) to dark coal (Soko, Rembas, Ćićevac) and stone coal (Rtanj, Podvis, Tresibaba). Such diversity of coal in Serbia is the result of favourable palaeographic conditions during the Neogene period, when large number of lakes with developed vegetation existed, including: Kolubara basin, Čačak-Kraljevo basin, Kostolac basin, Aleksinac basin, etc. Today, in Serbia, coal production is dominantly based on lignite exploitation at two locations: Kolubara coal basin and Kostolac coal basin (Fig. 2a). Lignite from these mines is used for the work of thermal powerplants TENT A and TENT B in Obrenovac (from Kolubara basin) and Drmno near Kostolac (from Kostolac basin). These thermal powerplants produce approximately 70% of electric energy in Serbia, so enabling the continuous work of these powerplants is of national interest and importance.

In this paper we present results of the research on optimization of the work of bucket-wheel excavators (BWEs), which are commonly used for open-pit coal mining in Serbia. For example, there are different types of excavators currently operating in Kolubara and Kostolac basin: Sch Rs 1400, Srs 1200, Srs 1300, Srs 2000, SchRs 630 and SchRs 900. Use of BWEs for open-pit coal mining is also common in other European countries, e.g., BWEs of type KU 300.S and KU 800 are used for mining in north Bohemia Basin [2]. Moreover, lignite in Greece is mainly extracted by continuous operation of BWEs, belt conveyors and spreaders [3]. Also, outside the Europe, in Australia, for instance, BWEs are mostly used for overburden removal [4].

The idea of optimization of the work of BWE due to different environmental working conditions is not new. One of the oldest attempts in this direction was made by Mashkovich and Fedorov [5], who analysed the dependence of the radial, lateral and peripheral component of the coal cutting force and energy consumption on the thickness and cross-sectional area of the

slice. The overburden was assumed to be composed of hard rocks and cohesive soils. Results of their research indicate that energy consumption of the coal cutting is 20% higher comparing with cutting of vertical slices. Also, their results indicate that cutting force increases linearly with the thickness and cross-section area of the slice. Coleman and Fitzhardinge [7] established correlation among unconfined compressive strength, chisel cutting resistance and point load strength index. On the other hand, Inal [6] developed a new diggability index for BWEs, based on series of correlation among compressive rock strength, peak cutting force, cone indenter, depth of cut, wedge strength of rock, specific energy, shore hardness and tensile rock strength. Bolukbassi et al. [8] developed overburden material diggability classification based on the correlation between cutting specific energy and Ohrenstein & Koppel wedge test. Scheffler [9] analysed the possibility of predicting the cutting resistance as a function of rock structure parameters in case when exploitation is done using BWEs. Dey and Ghose [10] suggested a new rockmass classification system for surface miners, by analyzing the dependence of the cuttability on the following parameters: point load index, volumetric joint count, abrasivity, direction of cutting respect to major joint direction and machine power. Suryo et al. [11] applied finite element method to analyse stress distribution on excavator bucket teeth. Tomus et al. [12] applied reliability calculations to determine average using time for three types of cutting teeth. Menegaki et al. [13] used fuzzy cognitive map approach to analyse the effect of different factors on BWE's efficiency. Results obtained indicate that material diggability and slope stability have predominant impact on the efficiency of excavator.

In this paper we analyse the dependence of the efficiency of the excavator on the geomechanical properties of the overburden, for the case study of open-pit coal mine "Tamnava Eastern Field" in Serbia (Fig. 1b and Fig. 2). The main idea of the research was to capture the most significant factors affecting the efficiency of the excavator, in order to be able to propose a strategy for the optimized use of BWE, enabling in that way longer working life and reducing the costs for the repairment.

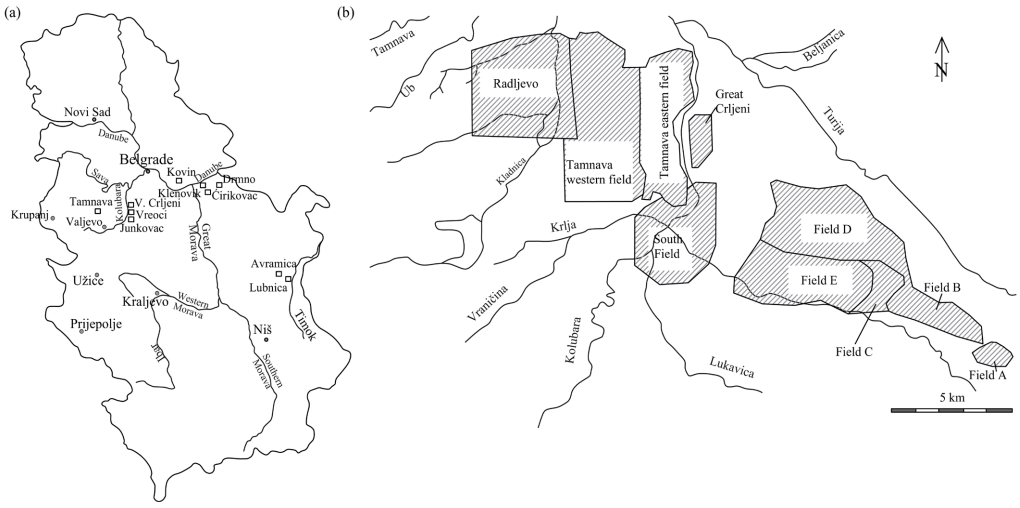

Fig. 2. (a) Distribution of open-pit coal mines in Serbia; (b) Distribution of the exploited open pits at the Kolubara mine

Unlike previous research on the efficiency of the BWE, the main idea of this research is to determine the significancy and nature of the effect of geomechanical properties on the overburden excavation process. The extensive analysis is done for different states of the excavator teeth: new and after 250 h of work, since engineering practice has shown that excavator teeth could show signs of significant deformation after 250 h of work. Analysis is conducted for the recorded values of the excavator current consumption I_{max} and velocity of the excavator rotary movement V_b, which are examined as functions of laboratory determined values of geomechanical factors (grain size composition, unit weight and shear strength). As we are aware, there are no previous attempts in establishing such correlations. Similar methodology was used in previous studies which established correlations between physical and mechanical soil and rock properties [14,15]. Using similar methods, Kostić et al. [16] analysed the effect of the main geomechanical properties of the Kovin coal on the linear and areal cutting resistance of the coal. Trivan et al. [17] developed explicit mathematical models, where cutting force and energy consumption are represented as the linear function of statistically significant influential factors: unit weight, compressive strength, and the cohesion of the overburden. Results obtained indicated that cutting force and energy consumption increases with the increase of unit weight, cohesion and compressive strength, while tensile strength and friction angle have statistically insignificant effect.

As far as authors are aware of, this is the first time such comprehensive analysis of the effect of overburden geomechanical properties on I_{max} and V_b is provided. No previous research provided explicit mathematical expressions indicating the correlation between the excavation parameters and geomechanical properties, which could further be used for actual prediction of the excavator work. Significance of the conducted research lies in the possibility of using developed models for prediction of the excavation process at the open-pit coal mine, which further optimize the process of the selection of the corresponding excavator and the assessment of its working life. On the other hand, the applied methodology could be used for other locations of overburden/coal excavation, where separate explicit models could be developed and used in practice.

The paper is organized in the following way. In Section 2 we describe the data analysed and methodology applied, while results of the research are given in Section 3. Geomechanical implications of the results obtained are analysed in Section 4. Section 5 is devoted to discussions and conclusions.

2. Methodology applied

In this paper we analyse data obtained for the overburden excavation at the ‘’Tamnava Eastern field’’ open-pit coal mine in Serbia. Data are collected for the case of overburden excavation with BWE of type SchRs 900 25/6, with the following characteristics: installed engine power for rotary wheel $Nm = 2 \times 230$ kW, geometric volume of bucket $q = 0.9$ m^3, number of buckets $z = 14$, number of emptying buckets per minute $n = 76$/min, angular distance between buckets 0.4488 rad, diameter of rotary wheel $D = 10.2$ m, length of rotary arrow $L_s = 35$ m, perimeter velocity of rotary wheel $V_k = 2.89$ m/s [18]. Cutting resistance was measured by recording the power of the bucket wheel, i.e. maximum current consumption I_{max} (A), velocity of the excavator rotary movement v_b (m/min), cut height h (m) and cut thickness s (m). We analyse the effect of geomechanical factors on I_{max} and V_b (Table 1). According to common relations Eqs (1)-(3), maximum energy consumption (KWh/m^3), linear and areal cutting resistance are directly propor-

tional to the current consumption. On the other hand, maximum energy consumption is inversely proportional to the current consumption. All the relevant cutting resistance parameters, namely, maximum energy consumption $E_{\max}$, areal cutting resistance $K_{F\max}$ and linear cutting resistance $K_{L\max}$ are inversely proportional to h and s:

$$E_{\max} = \frac{1.23 \cdot U \cdot I_{\max} \cdot \cos\varphi \cdot 0.001 \cdot \eta - N_{pr}}{60 \cdot h \cdot s \cdot V_b} \tag{1}$$

$$K_{L\max} = \frac{1.23 \cdot U \cdot I_{\max} \cdot \cos\varphi \cdot 0.001 \cdot \eta - \dfrac{60 \cdot h \cdot s \cdot V_b \cdot \gamma \cdot g \cdot h_d}{3600}}{V_b \cdot \sum_{i=1}^{m} L_i} \tag{2}$$

$$K_{F\max} = \frac{1.23 \cdot U \cdot I_{\max} \cdot \cos\varphi \cdot 0.001 \cdot \eta - \dfrac{60 \cdot h \cdot s \cdot V_b \cdot \gamma \cdot g \cdot h_d}{3600}}{V_b \cdot \sum_{i=1}^{m} F_i} \tag{3}$$

where $I_{\max}$ is the maximum current consumption of the excavator (A), V_b is the velocity of the excavator rotary movement (m/min), γ – unit weight of the excavated material (t/m^3), g is the gravity acceleration (m/s^2), h_d – height of the material lift up to the dump location (m), U is the rated voltage (V), cosφ is the power factor, determined from the engine characteristic curve (Fig. 3), h is the cut height (m) and s is the cut thickness (m), η represents coefficient of useful effect (0.925) N_{pr} – power of unloaded motion (11 kW), $\sum L_i$ – total length of the cutting edges in contact with material (cm), $\sum F_i$ – total area of cross-sections of the cut pieces (cm^2), m – total number of buckets which are in the same time in contact with material.

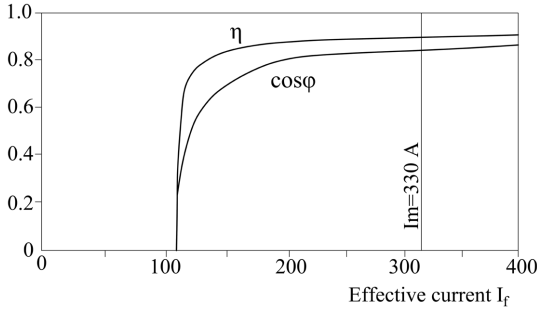

Fig. 3. Engine characteristic curve for the power of rotary wheel for excavator SchRs 900 25/6 (2 × 230 kW) used at "Tamnava Eastern Field": η – coefficient of useful effect, *cos*φ – power factor

This means that by analysing the dependence of $I_{\max}$ and V_b on geomechanical properties we can judge on the influence of geomechanical peroperties on the relevant cutting resistance parameters: $E_{\max}$, $K_{L\max}$ and $K_{F\max}$. Velocity of the excavator rotary movement V_b and the excavator current consumption $I_{\max}$ are chosen as dependent variable parameters since these parameters are actually measured on the excavator, and they are treated as measures of overburden cutting resistance.

Controlling and output factors which are analysed in this research are given in Table 1. Excavation data were collected form the mine directly, while geomechanical data were obtained as results of laboratory analyses. Heterogeneity of the geotechnical environment is taken into account by analyzing the range of values for grain size distribution, unit weight, cohesion and friction angle. In particular, overburden at the chosen location is composed of dominantly silty material, with occasionally increased amount of clay/small-grained sand. As one can see from Table 1, unit weight and cohesion have a significant range of values, while friction angle exhibits small variation.

TABLE 1

Overview of the analysed parameters and their range of values

New arrow excavator teeth	
Output factors	Range of values
I_{max} maximum current consumption (A)	592-920
V_b velocity of the rotary movement of the excavator (m/min)	13-24
Controlling factors	Range of values
CL_{per} percentage of clay in overburden (%)	5-45
SI_{per} percentage of silt in overburden (%)	43-91
SSN_{per} percentage of small-grained sand in overburden (%)	2-61
MSN_{per} percentage of moderate-grained sand in overburden (%)	1-8
γ unit weight of the overburden (kN/m^3)	16-22
c overburden cohesion (kPa)	19-25
φ overburden angle of internal friction (°)	22-23
Worn-out arrow excavator teeth after 250 h of work	
Output factors	Range of values
I_{max} maximum current consumption (A)	656-1000
V_b velocity of the rotary movement of the excavator (m/min)	13-24
Controlling factors	Range of values
CL_{per} percentage of clay in overburden (%)	4-45
SI_{per} percentage of silt in overburden (%)	44-92
SSN_{per} percentage of small-grained sand in overburden (%)	1-65
MSN_{per} percentage of moderate-grained sand in overburden (%)	1-8
γ unit weight of the overburden (kN/m^3)	16-22
c overburden cohesion (kPa)	19-25
φ overburden angle of internal friction (°)	22-23

Performed research consisted of three parts: field part included the collection of the recordings of I_{max} and V_b made at the excavator, and collection of undisturbed overburden samples. Current consumption I_{max} and velocity of the rotary movement of the excavator V_b were measured directly at the excavator. Laboratory part included determination of values of geomechanical factors: grain size, unit weight and shear strength, using the standard laboratory methods: grain size analysis using sieve and hydrometer, unit weight using the cylinder of known volume and shear strength in a direct shear test. Numerical part involved thorough statistical analysis of the obtained laboratory results, including the basic statistical approach, ANOVA test and multiple linear regression.

3. Results

3.1. New excavator teeth

Results of the performed analysis are shown in the following expressions (Table 2):

$$V_b = -553.08 - 0.025 \cdot CL_{per} + 0.178 \cdot SI_{per} + 1.596 \cdot SSN_{per} + 1.891 \cdot MSN_{per} + \\ + 25.08 \cdot \gamma - 5.09 \cdot c + 29.604 \cdot \varphi - 0.0296 \cdot SI_{per} \cdot MSN_{per} + \\ + 0.038 \cdot SSN_{per} \cdot c - 0.107 \cdot SSN_{per} \cdot \varphi + 0.208 \cdot \gamma \cdot c - 1.304 \cdot \gamma \cdot \varphi \quad (4)$$

$$I_{\max} = -12096.79 + 30.065 \cdot CL_{per} + 115.92 \cdot SI_{per} - 19.78 \cdot SSN_{per} + \\ - 182.77 \cdot MSN_{per} + 766.63 \cdot \gamma - 508.25 \cdot c + 621.79 \cdot \varphi + \\ - 0.165 \cdot CL_{per} \cdot SI_{per} + 1.149 \cdot CL_{per} \cdot \gamma - 1.77 \cdot CL_{per} \cdot c + \\ + 0.085 \cdot SI_{per} \cdot SSN_{per} - 5.006 \cdot SI_{per} \cdot \varphi - 0.597 \cdot SSN_{per} \cdot \gamma + \\ + 1.175 \cdot SSN_{per} \cdot c - 6.857 \cdot MSN_{per} \cdot \gamma + 13.871 \cdot MSN_{per} \cdot \varphi + \\ + 4.882 \cdot \gamma \cdot c - 37.486 \cdot \gamma \cdot \varphi + 18.619 \cdot c \cdot \varphi \quad (5)$$

where all parameters are explained Table 1.

TABLE 2

Results of ANOVA tests for models (4)-(5)

Model (4)				Model (5)			
Factors	**Sum of squares**	***F* value**	***p* value**	**Factors**	**Sum of squares**	***F* value**	***p* value**
CLper	2.840	0.383	0.541	CLper	8106.801	5.505	0.0294
SIper	15.209	2.051	0.164	SIper	22343.33	15.173	0.0009
SSNper	3.430	0.462	0.502	SSNper	2408.977	1.636	0.2155
MSNper	2.514	0.339	0.565	MSNper	87.28346	0.0592	0.8101
γ	11.362	1.532	0.227	γ	7508.749	5.099	0.0353
c	1.947	0.262	0.613	c	40.47598	0.0274	0.8700
φ	12.510	1.687	0.205	φ	10835.7	7.359	0.0134
SIper · MSNper	23.992	3.235	0.083	CLer · SIper	18675.28	12.682	0.0020
SSNper · c	61.423	8.281	0.0077	CLper · γ	14557.72	9.886	0.0051
SSNper · φ	34.636	4.670	0.040	Clper·c	36069.69	24.495	<0.0001
$\gamma \cdot c$	20.408	2.751	0.109	SIper·SSNper	14423.96	9.795	0.0053
$\gamma \cdot \varphi$	50.655	6.829	0.015	SIper · φ	27143.13	18.433	0.0004
Residual	200.27			SSNper · γ	9710.659	6.595	0.0184
				SSNper · c	44092.04	29.943	<0.0001
				MSNper · γ	18829	12.787	0.0019
				MSNper · φ	6232.796	4.233	0.0529
				$\gamma \cdot c$	11426.43	7.760	0.0114
				$\gamma \cdot \varphi$	26797.54	18.198	0.0004
				$c \cdot \varphi$	8617.625	5.852	0.0252
				Residual	29450.56		

Statistical analyses indicated high value of correlation coefficient and small values of RMSE: $R = 0.7$, RMSE = 2.24 (for Eq. 4) and $R = 0.94$, RMSE = 27.10 (for Eq. 5). It is clear from normal plots of residuals in Fig. 4 that error terms are normally distributed.

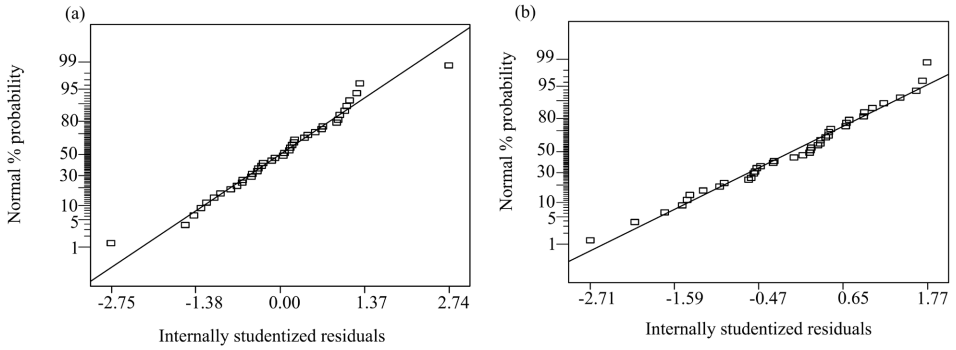

Fig. 4. Normal probability plots of residuals for Eq. 4 (a) and Eq. 5 (b)

As it could be seen from Table 2, individual factors have no significant effect on velocity of excavator rotary movement. However, significant two-factor interactions are obtained and shown in Fig. 5. Percentage of sand and silt, unit weight and shear strength parameters are singled out as the parameters with statistically significant two-factor interactions. It seems that higher values of V_b are obtained for the lower values of c and higher values of φ. On the other hand, nature

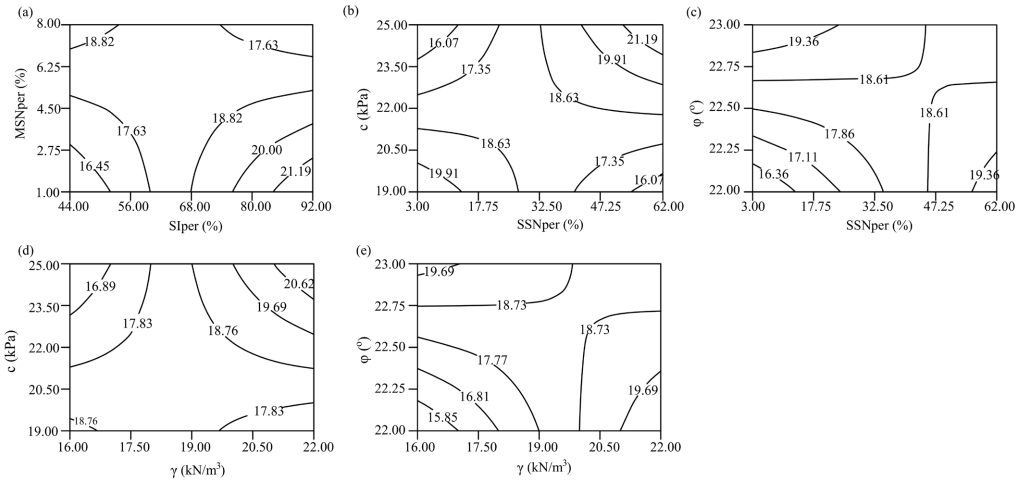

Fig. 5. Statistically significant two-factor interactions indicating influence of overburden mechanical properties on the velocity of the excavator rotary movement V_b – case of new excavator teeth: (a) $V_b = f$(MSNper, SIper); (b) $V_b = f(c$, SSNper); (c) $V_b = f(\varphi$, SSNper); (d) $V_b = f(c, \gamma)$; (e) $V_b = f(\varphi, \gamma)$. While a single parameter is varied, other parameters are being held constant at the following values: CLper = 24.5%, SIper = 68%, SSNper = 33.5%, MSNper = 4.5%, $\gamma = 19$ kN/m^3, $c = 22$ kPa, $\varphi = 22.5°$. Isolines represent values of excavator rotary movement

of the effect of γ and percentage of small-grained sand depends on the values of shear strength parameters: for lower values of cohesion, increase of γ leads to decrease of V_b, while for low values of φ – increase of γ leads to the increase of V_b. Both silt percentage and percentage of moderate-grained sand have positive effect on V_b.

As for the current consumption I_{max}, results obtained indicate that statistically significant factors CLper, SIper, γ and φ have strong individual positive impact, i.e., the increase of the content of clay and silt and their γ and φ leads to the increase of I_{max}.

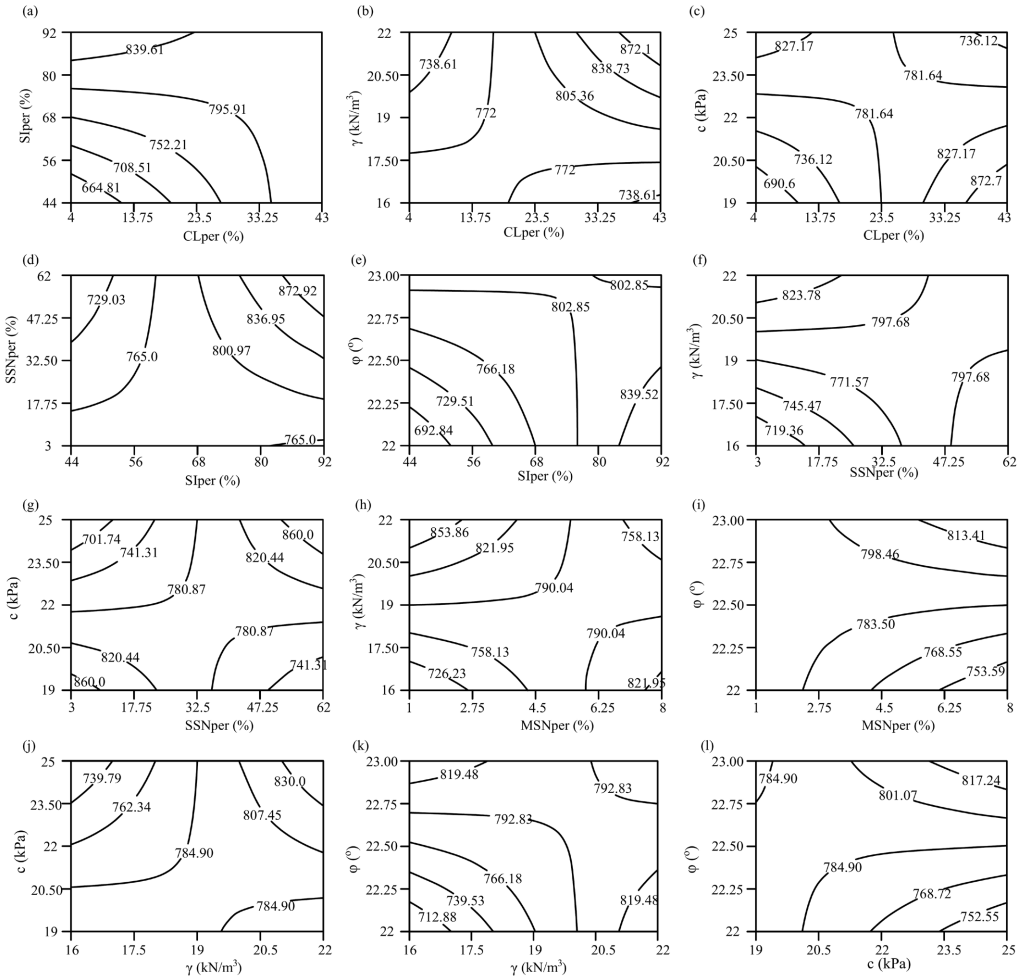

Fig. 6. Statistically significant two-factor interactions indicating influence of overburden mechanical properties on the excavator current consumption I_{max} – case of new excavator teeth: (a) $I_{max} = f$(SIper, CLper); (b) $I_{max} = f(\gamma$, CLper); (c) $I_{max} = f(c$, CLper); (d) $I_{max} = f$(SSNper, SIper); (e) $I_{max} = f(\varphi$, SIper); (f) $I_{max} = f(\gamma$, SSNper); (g) $I_{max} = f(c$, SSNper); (h) $I_{max} = f(\gamma$, MSNper); (i) $I_{max} = f(\varphi$, MSNper); (j) $I_{max} = f(c, \gamma)$; (k) $I_{max} = f(\varphi, \gamma)$; (l) $I_{max} = f(\varphi, c)$. While a single parameter is varied, other parameters are being held constant at the following values: CLper = 24.5%, SIper = 68%, SSNper = 33.5%, MSNper = 4.5%, $\gamma = 19$ kN/m^3, $c = 22$ kPa, $\varphi = 22.5°$. Isolines represent values of excavator current consumption

Besides the impact of these individual factors on I_{max}, performed analyses indicate the existence of statistically significant two-factor interactions. As one could see from Fig. 6, the significant two-factor interactions are the following:

– Grain-size composition:
  - Effect of clay percentage depends on the type of other factor in interaction. In particular, clay percentage has positive impact on I_{max} for moderate to high values of γ and for low to moderate values of cohesion. Increase of both clay and silt percentage leads to increase of I_{max};
  - Effect of silt percentage depends on the small-grained sand percentage – for low values of small-grained sand, increase of silt percentage leads to decrease of I_{max}. In all other interactions with clay percentage and φ – increase of silt percentage leads to the increase of I_{max};
  - Increase of small-grained sand percentage leads to decrease of I_{max} for low to moderate values of silt percentage and cohesion. Positive effect of small-grained sand percentage is independent of the overburden unit weight;
  - Effect of moderate-grained sand percentage is negative for moderate to high values of γ, and for low to moderate values of φ.

– Geomechanical properties:
  - Impact of overburden unit weight depends on the nature of the factor in the interaction. Negative effect of γ is observed for low to moderate values of clay percentage and for high values of φ. In all other cases, I_{max} increases with the increase of overburden unit weight;
  - Nature of the influence of overburden cohesion is similar to the effect of γ. Negative effect of cohesion on I_{max} is observed for high clay percentage and for low to moderate values of γ, φ and small-grained sand percentage;
  - Impact of φ on I_{max} is positive in all statistically significant interactions.

3.2. Worn-out excavator teeth after 250h of work

In case when excavation is performed with worn-out excavator teeth, the analysis indicates no significant correlation between the overburden geomechanical properties and velocity of excavator rotary movement. This means that V_b is independent of the overburden geomechanical properties in case of worn-out excavator teeth.

On the other side, certain correlation between the overburden geomechanical properties and current consumption I_{max} can be achieved (Table 3):

$$\begin{aligned} I_{\max} = & -392.34 + 38.42 \cdot CL_{per} - 36.83 \cdot SI_{per} + 35.44 \cdot SSN_{per} + \\ & - 3.92 \cdot MSN_{per} + 59.39 \cdot \gamma + 60.83 \cdot c + 3.97 \cdot \varphi + \\ & - 1.69 \cdot CL_{per} \cdot \varphi + 1.67 \cdot SI_{per} \cdot \varphi + 0.54 \cdot SSN_{per} \cdot \gamma + \\ & - 2.04 \cdot SSN_{per} \cdot \varphi - 3.29 \cdot \gamma \cdot c \end{aligned} \tag{6}$$

where meaning of all parameters is the same as for Eqs. (4) and (5) (Table 1).

Statistical analyses indicated lower value of correlation coefficient and higher values of RMSE compared to the case with new excavator teeth: $R = 0.64$, RMSE = 44.4 (for Eq. 6). It is clear from normal plots of residuals in Fig. 7 that error terms are normally distributed.

TABLE 3

Results of ANOVA tests for model (6)

Factors	Sum of squares	*F* value	*p* value
CLper	1550.75	3.34	0.0010
SIper	5999.13	0.64	0.4257
SSNper	146.47	2.49	0.1200
MSNper	5721.26	0.061	0.8062
γ	6273.15	2.37	0.1288
c	741.61	2.60	0.1120
φ	850.23	0.31	0.5812
CLper · φ	8195.72	0.35	0.5549
SIper · φ	8289.71	3.40	0.0702
SSNper · γ	18253.45	3.44	0.0687
SSNper · φ	15693.54	7.57	0.0079
$\gamma \cdot c$	10125.86	6.51	0.0133
Residual	1.422E+005		

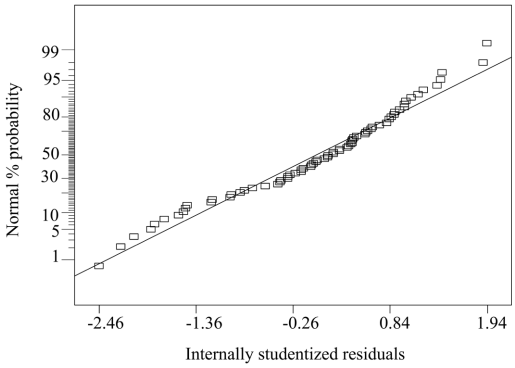

Fig. 7. Normal probability plots of residuals for Eq. (6)

As for the current consumption, results obtained indicate that statistically significant factors CLper, SIper, γ and φ have strong individual positive impact on I_{max}, i.e., the increase of the content of clay and silt and their γ and φ leads to increase of current consumption of the excavator. Besides this impact of the individual factors on I_{max}, as one could see from Fig. 8, there are statistically significant two-factor interactions, which indicate the following:

- Moderate-grained sand percentage does not enter any significant two-factor interaction;
- Clay and small-grained sand percentage have negative effect on I_{max} for high φ, while silt percentage have positive impact on I_{max} regardless of φ. Also, small-grained sand percentage has negative impact on I_{max} for low to moderate values of overburden unit weight;
- Cohesion has negative effect on I_{max} for high values of γ, while φ has negative impact on current consumption for low to moderate values of silt percentage and for moderate to high values of clay and small-grained sand percentage.

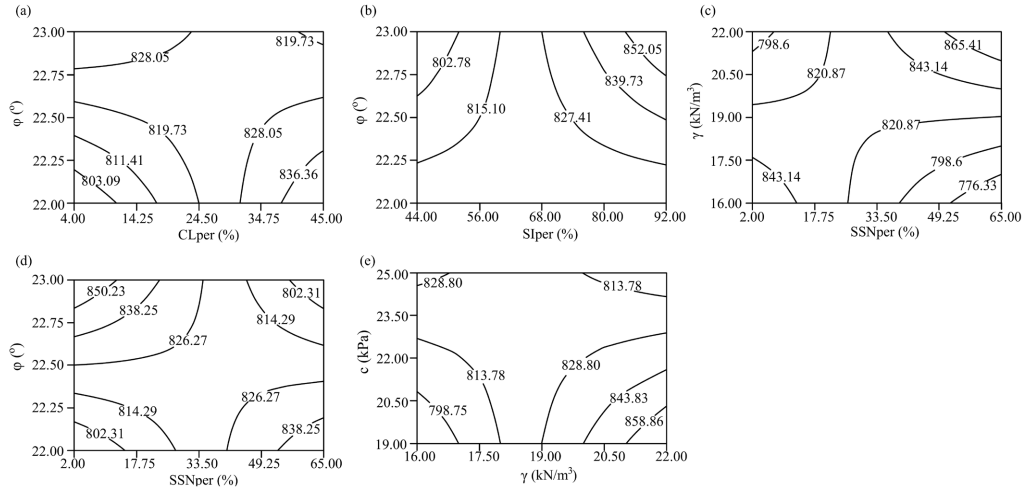

Fig. 8. Statistically significant two-factor interactions indicating influence of overburden mechanical properties on the excavator current consumption I_{max} – the case of worn-out excavator teeth after 250 h of work: (a) $I_{max} = f(\varphi,\text{CLper})$; (b) $I_{max} = f(\varphi,\text{SIper})$; (c) $I_{max} = f(\gamma,\text{SSNper})$; (d) $I_{max} = f(\varphi,\text{SSNper})$; (e) $I_{max} = f(c,\gamma)$. While a single parameter is varied, other parameters are being held constant at the following values: CLper = 24.5%, SIper = 68%, SSNper = 33.5%, MSNper = 4.5%, γ = 19 kN/m^3, c = 22 kPa, φ = 22.5°. Isolines represent values of excavator current consumption

4. Geomechanical implications

Analyses performed indicate that statistically significant effect of overburden grain-size composition and its geomechanical properties exists both for new and worn-out excavator teeth. Although the quality and quantity of these impacts is unambiguously proved by extensive statistical analyses, these effects should also have physical, and, consequently, geomechanical meaning. From the geomechanical viewpoint, one could explain the determined impact of the observed factors on the excavation parameters in the following subsections.

4.1. New excavator teeth: wheel velocity

Results obtained indicate that the overburden unit weight exhibits statistically significant two-factor interactions with shear strength parameters. Regarding the co-effect with cohesion, for low to moderate values of γ (16-19 kN/m^3), which correspond to overburden with predominant clayey particles, increase of γ leads to increase of V_b, indicating that more power is needed for heavier overburden particles (Fig. 9a). Regarding the interaction with angle of internal friction, positive effect of γ on V_b is almost independent of φ (Fig. 9b).

Overburden cohesion enters the significant interaction with percentage of small-grained sandy particles (SSNper) and unit weight. For low to moderate SSNper, increase of cohesion leads to decrease of V_b, meaning that less velocity is required for overburden with higher cohesion (Fig. 10a). This could be explained by the increased silt/clay percentage, where cohesion is mostly achieved on the account of pore water bonds. Similar co-effect is also observed for low to moderate values of γ (Fig. 10b).

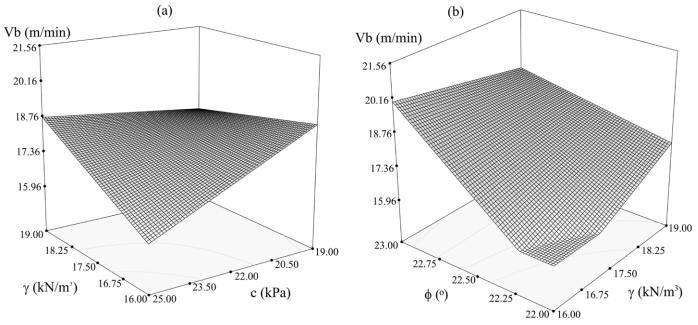

Fig. 9. Dependence of rotary excavator velocity V_b on the co-effect of overburden unit weight γ, and (a) overburden cohesion c, and (b) overburden angle of internal friction φ, for the case of new excavator teeth

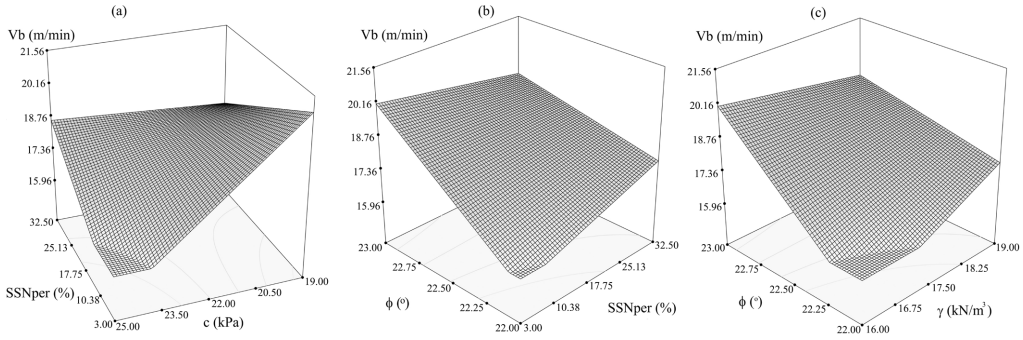

Fig. 10. Dependence of rotary excavator velocity V_b on the co-effect of (a) overburden cohesion c and percentage of small-grained sand SSNper, (b) overburden angle of internal friction φ and SSNper, and (c) φ and unit weight γ, for the case of new excavator teeth

Similarly to cohesion, angle of internal friction enters the significant two-factor interaction with γ and SSNper, but with the opposite impact on V_b. In particular, for low to moderate values of SSNper and γ, the increase of φ leads to increase of V_b (Figs 10b and 10c). This is expected, since higher φ requires more excavation power, which consequently leads to the increase of V_b.

Regarding the overburden grain-size distribution – the co-effect of SIper and MSNper is the only statistically significant two-factor interaction. It seems that the increase of silt percentage in overburden increases the excavator velocity V_b. At first glimpse, such effect of SIper on V_b is not expected, since the increase of silt percentage is commonly related to the increase of cohesion and decrease of φ, which means the reduction of V_b. However, such result could indicate that some other overburden property also significantly affects V_b. Such influence could be easily prescribed to overburden state of consistency (consistency index, I_c), or overburden compressibility properties. In particular, overburden in hard consistency state or with high compressibility modulus (which are the values that could be easily increased with the increase of silt percentage) could lead to increase of V_b.

4.2. New excavator teeth: current consumption

Regarding the effect of overburden unit weight interacting with grain-size distribution, in case for low to moderate percentage of small-grained sandy particles, increase of γ in the range 16-19 kN/m^3 (which is only meaningful, since low SSNper indicates higher percentage of clayey-silty particles, thus lower γ) leads to increase of Imax (Fig. 11a). For moderate to high values of SSNper, effect of γ on Imax is nearly independent of SSNper (Fig. 11b). This further means that the increase of γ leads to decrease of Imax only for silty-sandy overburden, while positive effect of γ on Imax is achieved for sandy-clayey overburden. Increase of γ indicates the increase of heavy sandy/silty particles, with little or no cohesion, which, in turn, requires smaller current consumption.

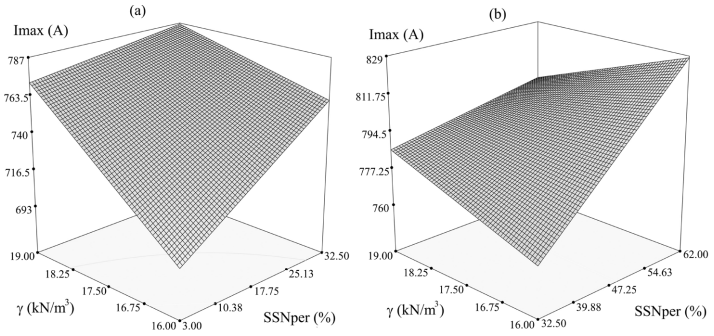

Fig. 11. Dependence of excavator current consumption I_{max} on the co-effect of overburden unit weight γ and (a) small-grained sand percentage SSNper (3-32,5%), (b) small-grained sand percentage, SSNper (32,5-62%), for the case of new excavator teeth

When overburden unit weight interacts with overburden shear strength parameters, unit weight positively effects on Imax for all values of cohesion and φ, except for the highest values of φ, which corresponds to predominantly sandy overburden, and which is compatible with the interaction of γ with the grain-size distribution.

As for the effect of overburden cohesion interacting with grain-size distribution in case of moderate to high values of clay percentage (which is only physically meaningful), increase of cohesion leads to decrease of I_{max} (Fig. 12a). Although this effect of cohesion on I_{max} could be seen as opposite to its real physical nature, this could be explained by the fact that cohesion in clayey overburden is achieved through the molecular bond of pore water and clay particles, which on macro level does not provide any significant resistance to excavation. This is confirmed by the statistically insignificant individual effect of cohesion on I_{max} (Table 2). The same effect of cohesion is observed for low to moderate percentage of small-grained sand (Fig. 12b).

When cohesion interacts with unit weight and angle of internal friction, for low to moderate values of γ, which are only relevant from the viewpoint of cohesion (cohesive clay particles commonly have lower values of γ), increase of cohesion leads to decrease of I_{max} (Fig. 13a). The same effect of cohesion on I_{max} is observed for low to moderate values of φ (Fig. 13b).

As for the effect of angle of internal friction, for low to moderate silt percentage, where range of φ = 22-23° is expected, increase of φ leads to increase of I_{max}, which is expected, since higher φ triggers stronger friction between the excavator and the overburden, leading to higher

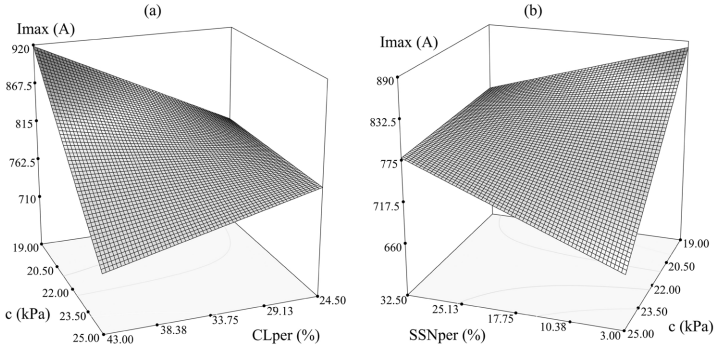

Fig. 12. Dependence of the excavator current consumption I_{max} on the co-effect of overburden cohesion c and (a) clay percentage in overburden, CLper, (b) small-grained sand percentage in overburden, SSNper, for the case of new excavator teeth

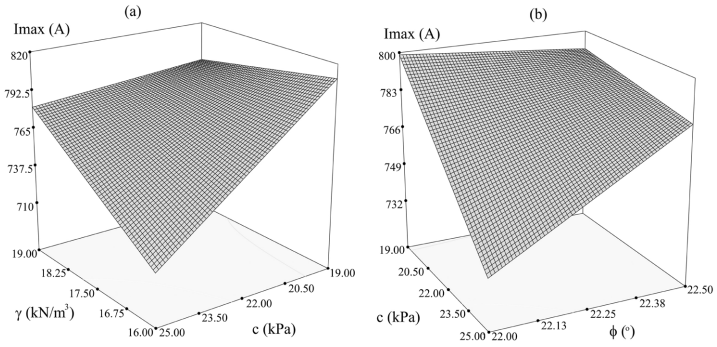

Fig. 13. Dependence of the excavator current consumption I_{max} on the co-effect of overburden cohesion c and (a) overburden unit weight γ, (b) overburden angle of internal friction φ, for the case of new excavator teeth

current consumption (Fig. 14a). Such effect of φ on I_{max} is observed regardless of moderate-grained sand percentage (Fig. 6). For low to moderate values of unit weight, where range of φ = 22-23° is expected, increase of φ leads to increase of I_{max} (Fig. 14b). Also, for all values of cohesion, increase of φ leads to higher current consumption (Fig. 6).

In case of effect of overburden grain-size distribution, for the examined ranges of clay and silt percentage, I_{max} increases with the increase of SIper and CLper. The effect of silt percentage on I_{max} is almost independent of the percentage of small-grained sand, in the range of SSNper up to 32.50%, which is the meaningful range for the examined value of γ (Fig. 6). On the other hand, for low values of SIper, increase of SSNper leads to decrease of I_{max}. Such effects of both examined two-factor interactions SIper and CLper and SSNper and SIper on I_{max} are not corresponding to the observed effects of cohesion and φ. One would expect that increase in SIper and CLper, which leads to increase in c and decrease in φ, causes also decrease in I_{max}. Similarly, it is expected that the increase in SSNper leads to increase in I_{max}. Such findings indicate that some other properties which were not examined also affect the excavator current consumption. One important property that could explain this dependence $I_{max} = f$(CLper · SIper, SIper · SSNper)

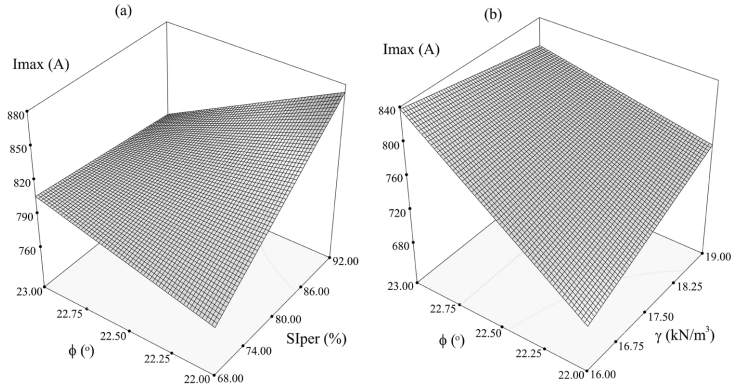

Fig. 14. Dependence of the excavator current consumption I_{max} on the co-effect of overburden angle of internal friction φ and: (a) silt percentage in overburden, SIper, (b) overburden unit weight γ, for the case of new excavator teeth

is the overburden compressibility and degree of consolidation. In case of overconsolidated clays and silt, which compose the overburden, with high values of compressibility modulus, increase in silt and clay percentage could lead to the increase of I_{max}. Similarly, when the increase of sand percentage indicates more compressible overburden, than I_{max} could really decrease with the increase of SSNper.

4.3. Worn-out excavator teeth: current consumption

The overburden cohesion enters the significant two-factor interaction only with overburden unit weight γ. For low to moderate values of γ, which correspond to predominantly silty-clayey overburden, increase of cohesion leads to increase of Imax (Fig. 15). This is an interesting finding, since for the case of new excavator teeth increase of cohesion leads to decrease of I_{max}. In analysed case, with worn-out excavator teeth, such results could indicate less excavation ability of worn-out excavator teeth, so more power-current consumption is required during the excavation.

Angle of internal friction of overburden exhibits significant co-effect with all overburden particles, except for the moderate-grained sand particles. Increase of φ leads to increase of I_{max} for all the relevant ranges of grain-size distribution: low to moderate values of CLper (Fig. 16a) and SSNper (Fig. 16b), and for moderate to high values of SIper (Fig. 16c). Such effect is expected since higher φ requires more excavation power, i.e., higher current consumption.

Overburden unit weight γ enters the significant two-factor interactions with cohesion and small-grained sand percentage. For all values of cohesion, increase of γ leads to increase of I_{max}. For low to moderate values of SSNper, increase of γ has almost no impact on I_{max}, which is expected, since there is no statistically significant interaction of γ with other soil fractions (Fig. 17a). For moderate to high values of SSNper, increase of unit weight leads to increase of I_{max}, since the increase of sand percentage in overburden commonly leads to increase of φ (Fig. 17b).

Regarding the co-effect of γ and cohesion, for low to moderate values of γ – increase of γ leads to increase of current consumption I_{max} for the examined range of values of cohesion (19-25 kPa), see Fig. 13.

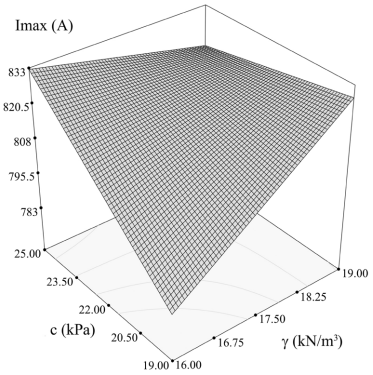

Fig. 15. Dependence of the excavator current consumption I_{max} on the co-effect of overburden cohesion c and unit weight γ, for the case of worn-out excavator teeth

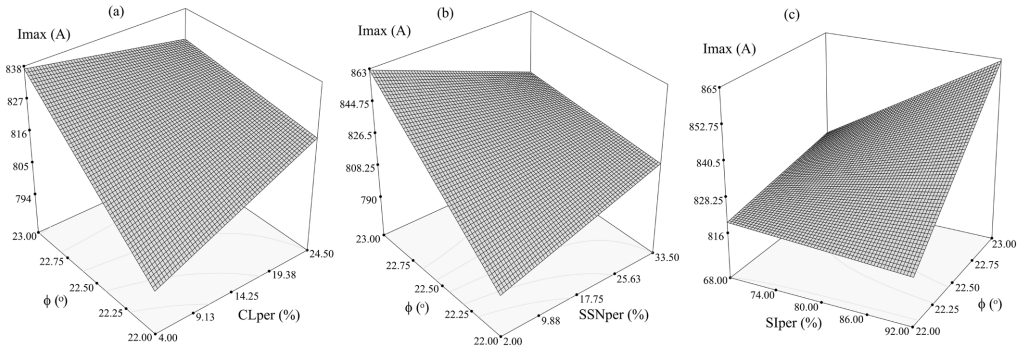

Fig. 16. Dependence of the excavator current consumption I_{max} on the co-effect of overburden angle of internal friction φ and: (a) clay percentage in overburden, CLper; (b) small-grained sand percentage in overburden, SSNper; (c) silt percentage in overburden, SIper, for the case of worn-out excavator teeth

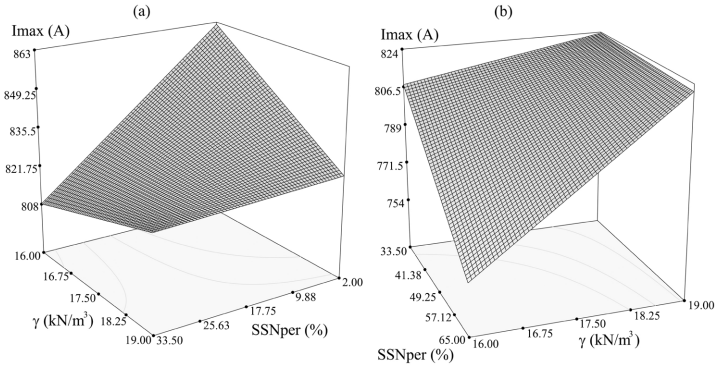

Fig. 17. Dependence of the excavator current consumption I_{max} on the co-effect of overburden unit weight γ and: (a) small-grained sand percentage in overburden, SSNper (2-33,5 %); (b) small-grained sand percentage in overburden, SSNper (33,5-65%), for the case of worn-out excavator teeth

5. Conclusions

In this paper we analyse the effect of geomechanical properties of overburden on the excavation parameters of BWE: current consumption I_{max} and velocity of excavator rotary movement V_b, for the open pit "Tamnava Eastern Field" case study in Serbia. The analysis is performed in order to optimize the excavation process in regard to overburden properties depending on the state of excavator teeth. Study conducted included the following overburden parameters: grain size distribution (percentage of clay, silt and sand), unit weight and shear strength parameters (cohesion and angle of internal friction), for two different states of excavator teeth: new and worn out after minimum of 250 h of work. Analysis is conducted using multiple linear regression approach, where excavation properties (I_{max} and V_b) are treated as nonlinear functions of the examined overburden properties. As a result, statistically significant geomechanical properties of the overburden are singled out, and their effect on I_{max} and V_b is thoroughly examined.

Results of the presented research could be used for optimization coal overburden excavation in order to reduce the current consumption by adjusting the excavator velocity depending on the geomechanical properties of the overburden. Based on derived models (4)-(6) one could estimate maximum current consumption I_{max} and rotary wheel velocity V_b solely by analyzing the geomechanical properties of the overburden.

Results of the conducted study indicate the following:

- Overburden properties almost entirely enter only the statistically significant two-factor interactions. The only exceptions are silt percentage, γ and φ which affect the current consumption for the case of new excavator teeth, and clay percentage which affects I_{max} for the case of worn-out excavator teeth;
- No statistically significant correlations could be obtained between the overburden properties and V_b for the case of worn-out excavator teeth. Also, there is no statistically significant effect of grain size distribution on I_{max} for the case of worn-out excavator teeth;
- Effect of unit weight is positive for almost all examined cases (V_b and I_{max} increases with the increase of γ), except for silty-sandy overburden, where I_{max} decreases with the increase of γ, probably due to low cohesion of silty-sandy material;
- Effect of φ on V_b and I_{max} is also positive for all examined cases;
- Effect of cohesion on V_b and I_{max} is negative for the case of new excavator teeth, i.e. increase of cohesion leads to decrease of I_{max}, which could be explained by the increased silt/clay percentage, where the cohesion occurs due to bonds between pore water and clay particles. However, cohesion has positive impact on I_{max} for the case of worn-out excavator teeth, which could indicate less excavation ability of worn-out excavator teeth, so more current consumption is required during the excavation;
- Effect of grain size distribution on V_b and I_{max} is such that the increase of silt percentage in overburden increases V_b and I_{max}, which could be explained by the strong impact of some other overburden property which was not examined, in this study, e.g., overburden consistency state, degree of consolidation or compressibility properties.

Besides the detailed analysis of the statistically significant factors affecting the current consumption and excavator rotary movement, performed analysis provided explicit mathematical expressions in a form of nonlinear function of I_{max} (both for the case of new and worn-out excavator teeth), and V_b (only for the case of new excavator teeth), and the significant overburden properties. These expressions enable reliable predictions of I_{max} and V_b before the start of exca-

vation, solely based on overburden properties, which enable optimization of the work of BWE. Such energy saving approaches are especially analysed in recent research, regardless of the type of the system observed [19,20].

In the context of the specific case study that has been analyzed, the obtained expressions provide accurate mathematical relations between the geomechanical parameters of the overburden and the excavation parameters, and, as such, could be used in further excavation activities. In general case, regarding the overburden excavation regardless of the specific site, the obtained expressions could be considered qualitatively, indicating the most significant individual factors and two-factor interactions which affect the excavation process. Also, the optimization procedure presented in this paper could be efficiently used in case of modern automated and unmanned machinery [21]. Moreover, the optimization of excavation procedure leads to reduction of dust and dump material, and, consequently, contributes to cleaner environment in surface coal mining [22].

Further research on this topic should include more overburden properties (e.g., compressibility modulus, consistency state, degree of consolidation), in order to scrutinize the effect of grain-size distribution (clay/silt percentage) on $I_{\max}$ and V_b. Moreover, similar approach could be used in case of hard rock overburden. Also, estimation models developed in this paper for $I_{\max}$ and V_b could be further evaluated for the newly recorded field data.

References

[1] S. Vujić et al. (Eds.), Serbian mining and geology in the second half of the XX century. 2014 Academy of Engineering Science of Serbia, Matica Srpska and Mining Institute, Belgrade.

[2] M. Hummel, Comparison of existing open coal mining methods in some countries over the world and in Europe. J. Min. Sci. **48**, 146-153 (2012). DOI: https://doi.org/10.1134/S1062739148010169

[3] K. Kavouridis, Lignite industry in Greece within a world context: mining, energy supply and environment. Energ. Policy **36**, 1257-1272 (2008). DOI: https://doi.org/10.1016/j.enpol.2007.11.017

[4] B. Scott, P.G. Ranjith, S.K. Choi, M. Khandelwal, A review on existing opencast coal mining methods within Australia. J. Min. Sci. **46**, 280-297 (2010). DOI: https://doi.org/10.1007/s10913-010-0036-3

[5] O.N. Mashkovich, D.I. Fedorov, Working hard rocks with a bucket-wheel excavator. Sov. Min. Sci. **4**, 49-52 (1968). DOI: https://doi.org/10.1007/BF02501984

[6] A. Inal, The development of diggability index for bucket wheel excavators. MSc Thesis, The University of New South Wales, School of Mining Engineering, Faculty of Applied Science, Sidney, Australia, (1984).

[7] J.R. Coleman, C.F.R. Fitzhardinge, Geotechnology of excavation equipment selection with particular emphasis on bucket wheel excavators. In: National conference publication – Institution of Engineers, Australia 1979.

[8] N. Bolukbassi, O. Koncagul, A. Gunhan Passamehmetoglu, Correlation of rock properties and cutting resistances in assessment of diggability with bucket-wheel excavators. T. In. Min. Metall A. **100**, 189-193 (1991).

[9] D. Scheffler, Laboratory and in-situ methods of measurement as the basis for predicting cutting resistances in mining machines. Zkg Int. **50** (7), 347-352 (1997).

[10] K. Dey, A.K. Ghose, Review of cuttability indices and a new rockmass classification approach for selection of surface miners. Rock Mech. Rock Eng. **44**, 601-611 (2011). DOI: https://doi.org/10.1007/s00603-011-0147-4

[11] S.H. Suryo, A.P. Bayuseno, J. Jamari, A. Imam Wahyudi, Analysis of Rake Angle Effect to Stress Distribution on Excavator Bucket Teeth Using Finite Element Method. Civil Engineering Journal-Tehran **3**, 1222-1234 (2017).

[12] O. Tomuș, A. Andraș, D. Jula, S. Dinescu, Aspects relating to the reliability calculation of the cutting-teeth mounted on the bucket wheel excavators used in lignite mining. MATEC Web Conf.Volume **290**, 9th International Conference on Manufacturing Science and Education – MSE 2019 "Trends in New Industrial Revolution" 01020, 1-8 (2019).

[13] M. Menegaki, T. Michalakopoulos, Exploring the effect of physical, human and technical factors on bucket wheel excavators' efficiency: a fuzzy cognitive map approach. Int. J. Min. Miner. Eng. **10**, 189-204 (2019). DOI: https://doi.org/10.1504/IJMME.2019.104447

[14] S. Kostić, N. Vasović, D. Jevremović, Stability of earth slopes under the effect of main environmental properties of weathered clay-marl deposits in Belgrade (Serbia). Environ. Earth Sci. **75**, 492, 1-10, (2016). DOI: https://doi.org/10.1007/s12665-016-5339-5

[15] S. Kostić, Analytical models for estimation of slope stability in homogeneous intact and jointed rock mass with a single joint. Int. J. Geomech. **17** (10), 04017089 (2017). DOI: https://doi.org/10.1061/(ASCE)GM.1943-5622.0000994

[16] S. Kostić, J. Trivan, N. Gojković, Estimation of coal cutting force based on the impact of geomechanical factors. In: V. Litvinenko (Ed.) EUROCK2018: Geomechanics and Geodynamics of Rock Masses, CRC Press, Taylor and Francis Group (2018).

[17] J. Trivan, S. Kostić, M. Šalović, Calibration of excavator cutting force and energy consumption considering the impact of the overburden mechanical properties. In: S. Vujić et al. (Eds.) Proceedings of VIII Balkanmine (2022) (in press).

[18] D. Ignjatović, Choice of the method for determining the cutting resistance using rotary bucket-wheel excavators in conditions of open pit lignite mines of Kolubara. MSc Thesis, University of Belgrade Faculty of Mining and Geology, Serbia (1993).

[19] M.A. Oskouei, K. Aquah-Offei, Statistical methods for evaluating the effect of operators on energy efficiency of mining machines. Mining Technology, Transactions of the Institutions of Mining and Metallurgy, Section A, **123**, 4, 1-8 (2014).

[20] H. Trenchard, M. Perc, Energy saving mechanisms, collective behavior and the variation range hypothesis in biological systems: A review. BioSystems **147**, 40-66 (2016).

[21] L. Dong D. Sun, G. Han, X. Li, Q. Hu, L. Shu, Velocity-free Localization of Autonomous Driverless Vehicles in Underground Intelligent Mines. IEEE Transactions on Vehicular Technology **69**, 9292-9303 (2020).

[22] L. Dong, X. Tong, X. Li, J. Zhou, S. Wang, B. Liu. Some developments and new insights of environmental problems and deep mining strategy for cleaner production in mines. Journal of Cleaner Production **210**, 1562-1578 (2018).